NTEC 11	(1) 38	Title

Core Design for Light Water Cooled Reactors

By

G.F.Hewitt

Imperial College, London

NTEC 11	(2) 38	Summary

NTEC 11	(3) 38	PWR Fuel

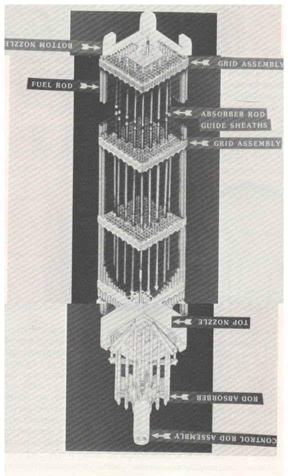

17X17 square pitch Bundle.
12 ft (3.66m) long

NTEC 11	(4) 38	BWR Fuel

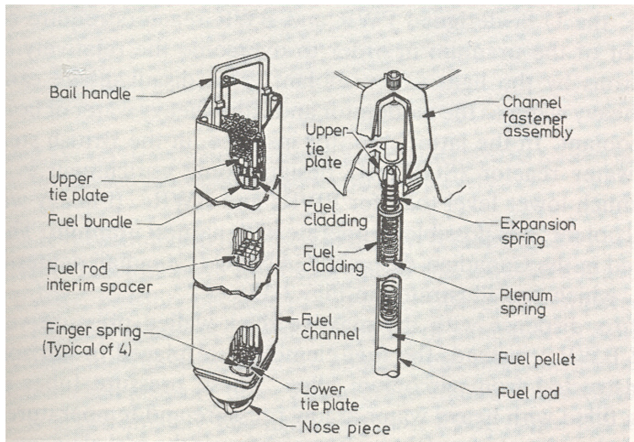

NTEC 11 | (5) 38

RMWR Fuel

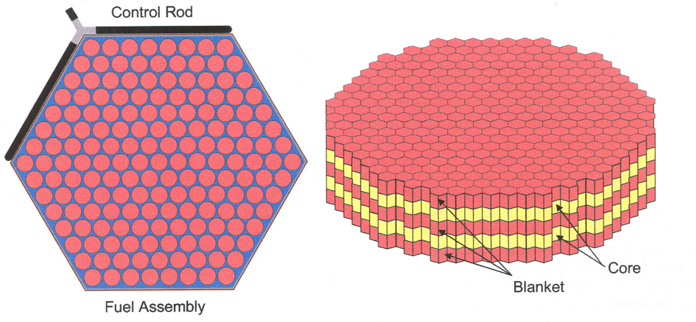

Reduced-moderation water reactor (RMWR)
Objective:Reduce water inventory and increase breeding

NTEC 11 | (6) 38

RMWR fuel assembly

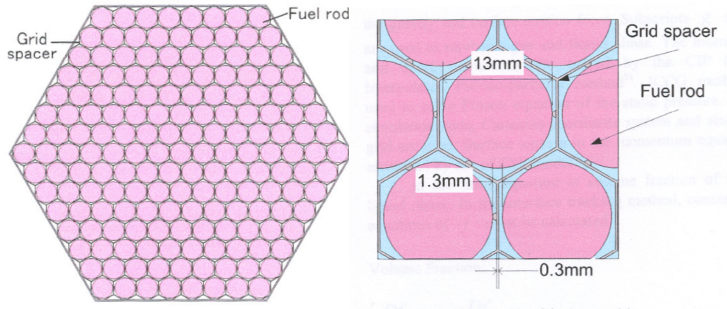

(a) Fuel assembly (b) Detail of fuel assembly

NTEC 11 | (7) 38

BARS core

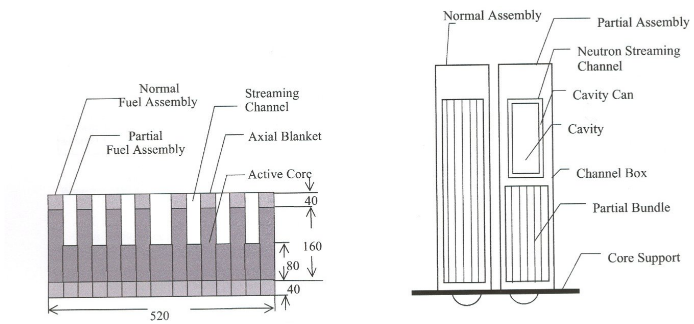

(a) Vertical view of BARS Core (b) Vertical view of fuel assembly

BARS – BWR with Advanced Recycle System

NTEC 11 | (8) 38

Lumped parameter CHF correlations

Lumped parameter correlation of Bertoletti et al (1965):

$$\frac{W_{Bh}}{\dot{M}h_{LG}} = \frac{P_h}{P_{tot}} \frac{1 - p/p_c}{0.1\dot{m}^{1/3}} \frac{L_B}{L_B + 0.1988(p_c/p - 1)D_e^{1.4}\dot{m}}$$

$$D_e = \frac{4A}{P_{tot}}$$

NTEC 11 | (9) 38

Seven rod bundle experiments with varying rod layouts

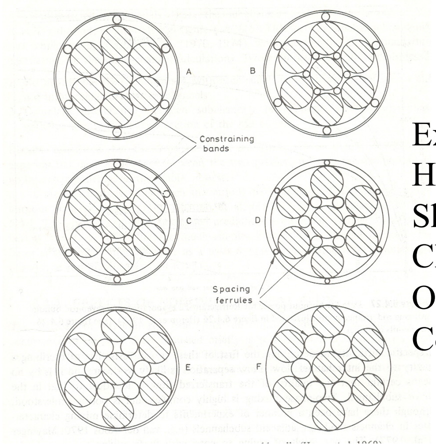

Experiments of Heron et al (1969): Should give same CHF value on basis Of lumped parameter Correlation.

NTEC 11 | (10) 38

Results from seven-rod bundle experiments

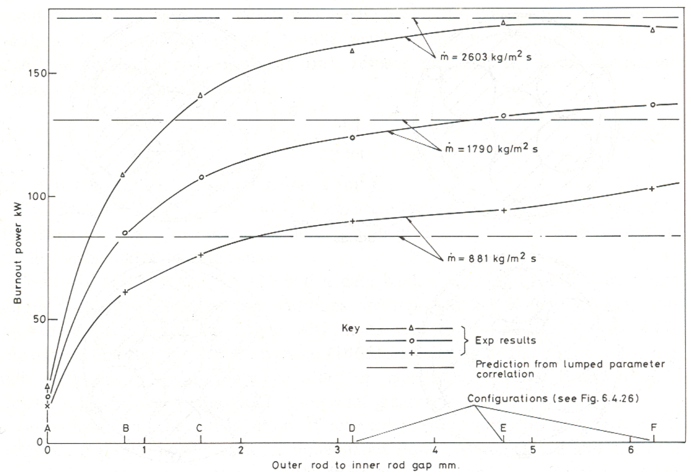

NTEC 11 | (11) 38

Types of sub-channel model

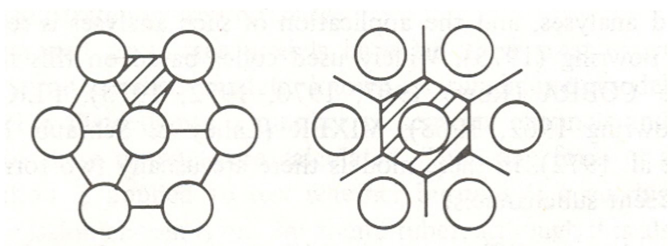

Channel-centred Sub-channels

Rod-centred Sub-channels

NTEC 11 | (12) 38

Channel-centred sub-channels

Modelling methodology:

(a) Takes account of transfer between sub-channels due to differences in pressure.

(b) Takes account of turbulent mixing between sub-channels

(c) Uses standard models such as drift flux to describe flows.

(d) Applies correlations of local heat flux/quality type bases on bundle data

Typical codes: COBRA, HAMBO, FLICA

NTEC 11	(13) 38	Application of channel-centred sub-channel model (Jeong et al. 2005 – MARS code)

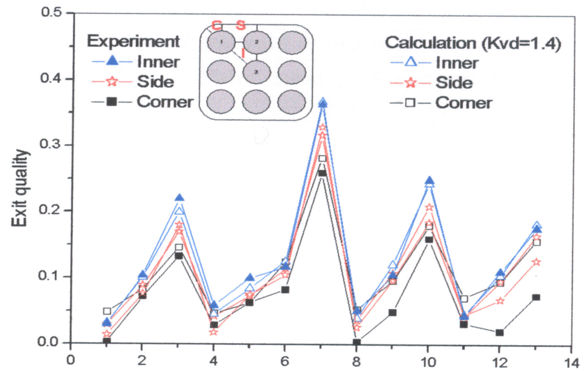

Prediction of outlet quality distribution for GE 9-rod bundle experiment for various conditions.

NTEC 11	(14) 38	Problems with q/x correlation strategy

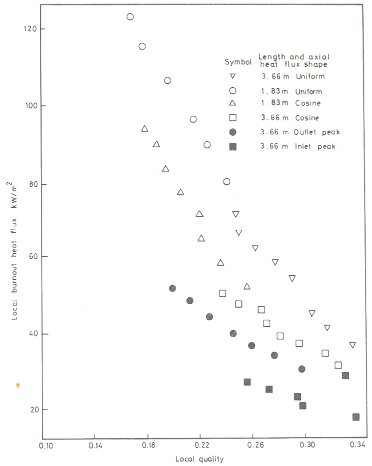

Non-uniform heat flux data not correlated by q/x form

Refrigerant 114 CHF data of Shiralkar (1972)

NTEC 11	(15) 38	Quality/boiling length correlation

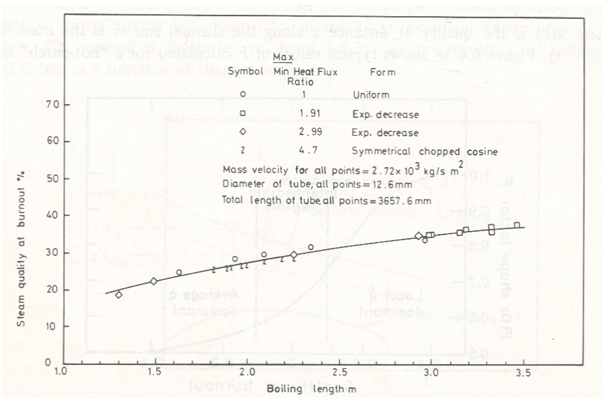

CHF data of Keeys et al)1971). Water at 6.89 MPa

NTEC 11	(16) 38	Rod centred sub-channels

Gaspari et al (1970, 1974)

Application of CISE quality/boiling length correlation for tubes:

$$x_{BO} = \frac{W_B}{\dot{M}h_{LG}} = \frac{1 - p/p_c}{0.1\dot{m}^{1/3}} \frac{L_B}{L_B + 0.1988(p_c/p - 1)D^{1.4}\dot{m}}$$

to each rod-centred sub-channel

NTEC 11	(17) 38	**Application of rod-centred sub-channel model (Gaspari et al, 1974)**

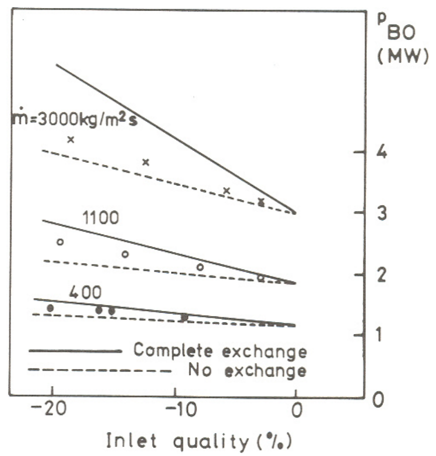

Two extreme cases:

(a) No mixing between adjacent rod-centred sub-channels.

(b) Complete interchange to give constant enthalpy at a given cross section of bundle

NTEC 11	(18) 38	**Three-fluid codes**

Recognising the need to consider the separate existence of film and drop liquid the three-fluid codes use channel centred sub-channels but have three fields (vapour, drops, liquid film).

Liquid film assumed to be same on all surfaces in sub-channel.

Fixed phase fraction assumed for flow pattern transitions
e.g. slug/churn at ε_G=0.50, churn/annular at ε_G=0.75, ε_{LF}=10^{-5} for CHF (dryout)

Typical codes: COBRA-TF, NASCA, TCAPE

NTEC 11	(19) 38	**Application of NASCA code to prediction of RMWR bundle (Tamai et al, 2003)**

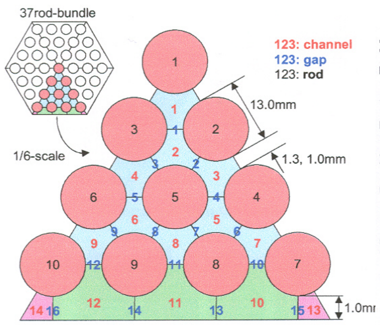

Sub-channel division

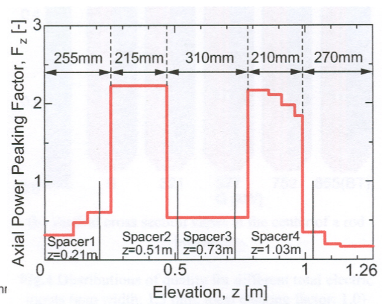

Axial heat flux profile

NTEC 11	(20) 38	**Results from RMWR bundle calculations with NASCA (Tamai et al, 2003)**

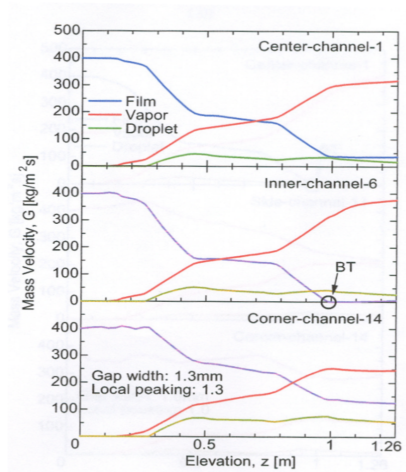

CHF ("Boiling Transition", BT) is predicted to occur in the inner channel.

NTEC 11	(21) 38	Post-dryout heat transfer in codes

Most codes use simplified equations:

Dougal-Rohsenow(1963) correlation:

$$\frac{\alpha D_H}{\lambda_{g,f}} = 0.023\left\{\frac{\dot{m}D_H}{\eta_{g,f}}\left[x_e + \frac{\rho_{g,s}}{\rho_{l,s}}(1-x_e)\right]\right\}^{0.8} \mathrm{Pr}_{g,f}^{0.4}$$

Groeneveld (1973) correlation:

$$\frac{\alpha D_H}{\lambda_{g,s}} = 0.00327\left\{\frac{\dot{m}D_H}{\eta_{g,s}}\left[x_e + \frac{\rho_{g,s}}{\rho_{l,s}}(1-x_e)\right]\right\}^{0.901} \times \mathrm{Pr}_{g,w}^{1.32}\left\{1.0 - 0.1\left(\frac{\rho_{l,s}}{\rho_{g,s}} - 1\right)^{0.4}(1-x_e)^{0.4}\right\}^{-1.50}$$

Problem: Non-equilibrium effects (Hewitt,1998)

NTEC 11	(22) 38	Transients: Extension of film dryout methodology (James and Whalley, 1978)

Equations for core and film:

$$\frac{\partial}{\partial t}\left[\rho_L(1-\varepsilon_{GC})\right] + \frac{\partial \dot{m}_{LF}}{\partial z} = \frac{4}{d}(D - E - \dot{q}/h_{LG} - F_{LF})$$ Film mass balance

$$\frac{\partial}{\partial t}\left[\rho_L \varepsilon_{GG}\varepsilon_d)\right] + \frac{\partial \dot{m}_{LE}}{\partial z} = \frac{4}{d}(E - D - F_{LE})$$ Core mass balance

$$\frac{\partial}{\partial t}\left[\rho_G \varepsilon_{GC}(1-\varepsilon_d)\right] + \frac{\partial \dot{m}_{G}}{\partial z} = \frac{4}{d}(\dot{q}/h_{LG} + F_{LF} + F_{LE})$$ Vapour mass balance

$$\frac{\partial}{\partial t}\left[\rho_L e_{iL}(1-\varepsilon_{GC}) + \rho_L e_{iL}\varepsilon_{GC}\varepsilon_d + \rho_G e_{iG}\varepsilon_{GC}(1-\varepsilon_d)\right] + \frac{\partial}{\partial z}(h_L\dot{m}_{LF} + h_L\dot{m}_{LE} + h_G\dot{m}_G) = \frac{4\dot{q}}{d}$$

Overall energy balance

F_{LF} and F_{LE} are the rates of flashing of the film and drops per unit interface area

e_{iL} and e_{iG} are the internal energies of the liquid and vapour phases

NTEC 11	(23) 38	Prediction of Moxon and Edwards (1967) Transient data (Hewitt & Govan, 1990)

Inlet mass flux varies with time according to equation:

$$\dot{m}(t) = 786 + 1926\exp(-t/0.275)$$

Run No.	Heat flux (kW/m²)	Subcooling (kJ/kg)	Time to dryout (s)			
			Experiment	Old Model (PWJ1)	New Model (PWJ1A)	New model pseudo steady-state
45/276	955	58.15	0.95	0.65	0.80	0.36
45/275	960	53.50	0.89	0.63	0.77	0.34
45/286	1155	46.52	0.40	0.34	0.37	0.08
45/284	1174	58.15	0.30	0.34	0.35	0.07

NTEC 11	(24) 38	Dryout and rewetting I: Hewitt and Govan (1990)

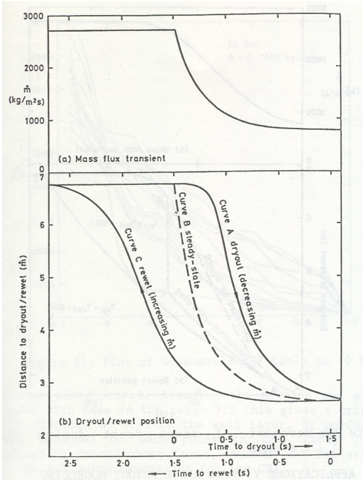

Transitions occur when film flow rate at wet/dry boundary is zero as calculated from transient film flow model.

NTEC 11	(25) 38	Dryout and rewetting II: Hewitt and Govan (1990)

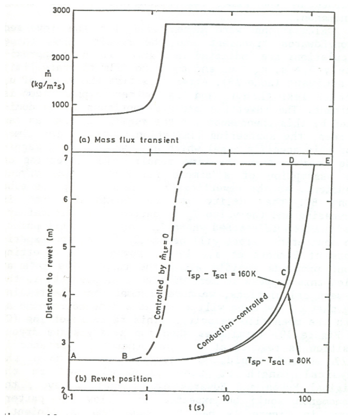

(a) Fast transient

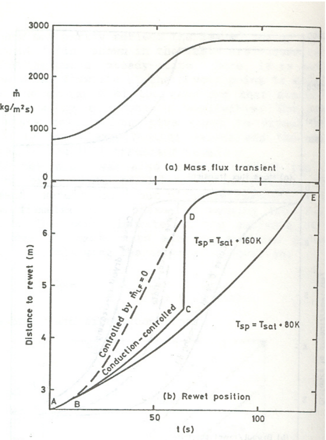

(b) Slow transient

NTEC 11	(26) 38	Prediction of dryout, post-dryout and rewetting with TCAPE (Ishida et al, 2003)

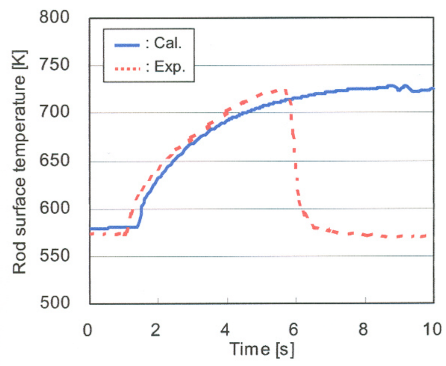

Prediction of 9X9 bundle. Spacer grid effects?

NTEC 11	(27) 38	Rod film bookkeeping I: Annulus with bilateral heating (Whalley et al, 1974)

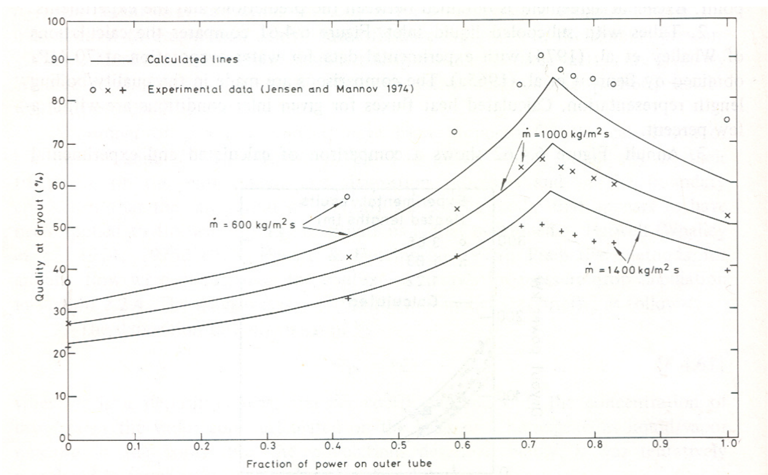

NTEC 11	(28) 38	Rod film bookkeeping II: 37-rod bundle (Whalley et al, 1974)

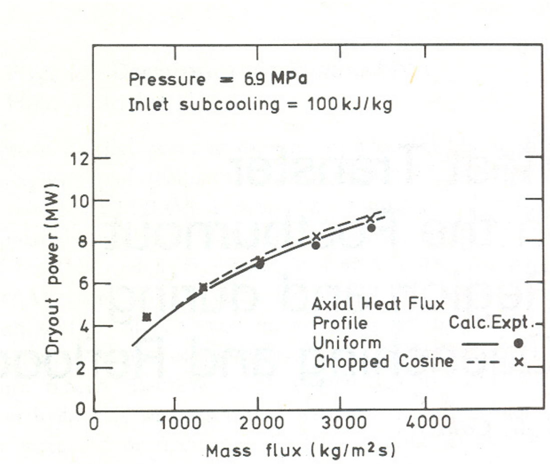

NTEC 11	(29) 38	**Effect of heat flux (Ng, 1996): Prediction of 3X3 rod bundle**

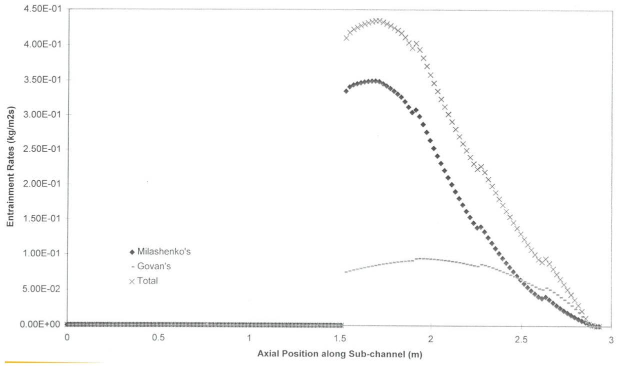

The Milashenko correlation gives main contribution to the entrainment rate. Doubtful validity. Experiments of Adamsson and Anglart (2005) confirm that heat flux effect is weak.

NTEC 11	(30) 38	**Droplet deposition by direct impaction**

Droplets deposit by diffusion and by direct impaction (James et al, 1980).

For tubes, all droplets finally deposit on surface from which they originated. For annuli and rod bundles, droplets may “leak” to unheated surfaces and thus there is an apparent increase in transfer away from the heated surface.

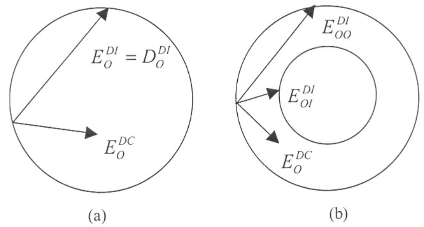

Anglart and Adamsson (2003) Prediction of annulus film flow rate data and dryout taking account of direct Impaction.

NTEC 11	(31) 38	**Prediction of data of Moeck (1970) for film flows in an annulus**

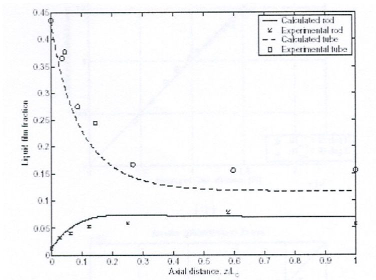

P=34.5 bar, *x* = 0.31

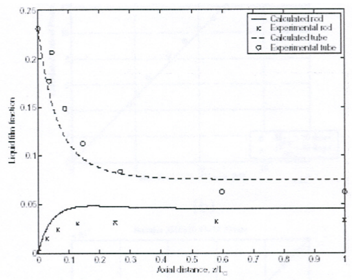

P=34.5 bar, *x*=0.39

Calculations by Anglart and Adamsson (2003)
Agreement improved by taking account of direct impaction.

NTEC 11	(32) 38	**Influence of spacer grids**

Vortex structure

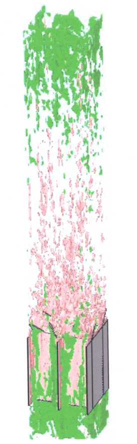

Velocity-fluctuation structure

Spacer grids have strong effect on turbulence and hence on droplet deposition processes downstream of the grids.

LES simulations of flow/spacer grid interactions: Ikeno and Kajishima (2005)

NTEC 11	(33) 38	Influence of grid obstacles on droplet deposition (Okawa et al. 2005)

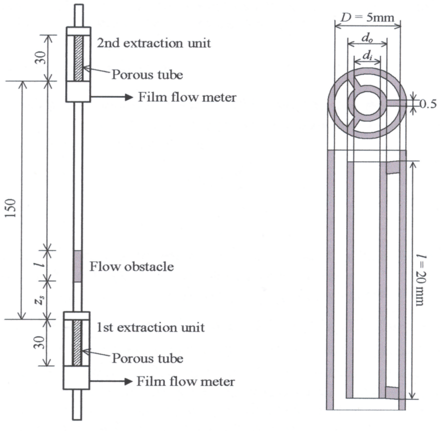

(a) Deposition Section (b) Flow Obstacle

Rate of droplet deposition measured with and without obstacle simulating spacer grid.

NTEC 11	(34) 38	Effect of grid-simulating obstacle on droplet deposition coefficient (Okawa et al (2005)

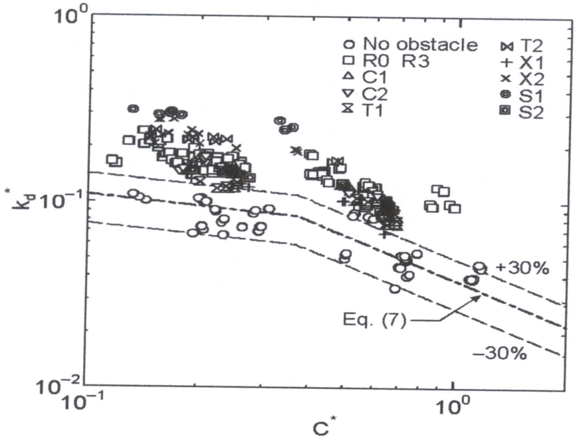

NTEC 11	(35) 38	Modelling of low quality dryout: Weisman and Pei (1983) model

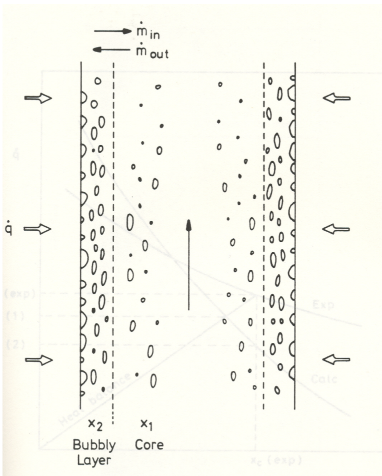

CHF condition corresponds to situation where:

$$\dot{q}_b = \dot{m}_{out}(x_2 - x_1)h_{LG}$$

Where q_b is that part of the heat flux which goes into generating bubbles.
Critical condition corresponds to void fraction in the wall layer of 0.82

NTEC 11	(36) 38	Application of Weisman model into core DNB prediction (Mitsuhashi et al, 2003)

Coupling of sub-channel analysis and three-dimensional two-fluid model.

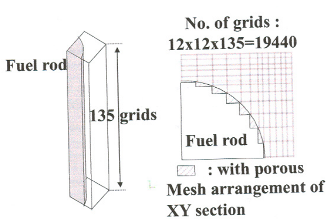

Mesh for 3-D multifluid model

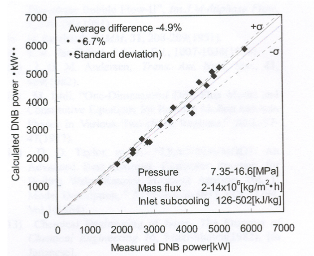

Comparison of predicted and measured DNB power

NTEC 11	(37) 38	**Full range CHF model (Hewitt and Govan, 1990)**

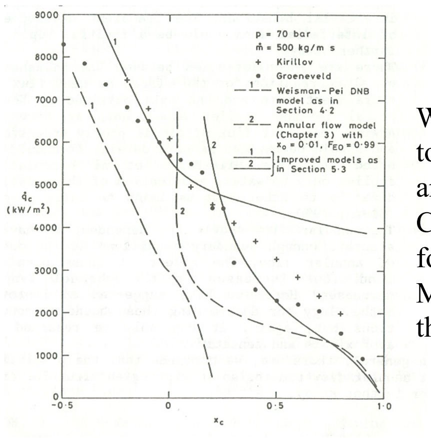

Weisman-Pei model adapted to apply to both sub-cooled and annular region.
Compared with look-up tables for CHF.
Model giving lowest CHF is the one that applies.

NTEC 11	(38) 38	**Conclusions**

- A wide variety of methods exists for prediction of fuel thermal hydraulic behaviour and in particular of CHF.
- Models which are phenomenological in nature are very promising but their application reflects current deficiencies in understanding droplet transport and other detailed processes.